

# Application of the Wolf method for the evaluation of Coulombic interactions to complex condensed matter systems: Aluminosilicates and water

Pierfranco Demontis, Silvano Spanu, and Giuseppe B. Suffritti<sup>a)</sup>  
*Dipartimento di Chimica, Università di Sassari, Via Vienna 2, I-07100 Sassari, Italy*

(Received 13 November 2000; accepted 20 February 2001)

The application of the method recently proposed by Wolf *et al.* [J. Chem. Phys. **110**, 8254 (1999)] for the evaluation of Coulombic energy in condensed state systems by spherically truncated, pairwise  $r^{-1}$  summation is verified for liquid water and anhydrous and hydrated aluminosilicates. Criteria for the estimation of the optimum values for the truncation radius and the damping parameter are discussed. By several examples it is verified that the new method is computationally more efficient than the traditional Ewald summations. For the considered systems the performances of the new method are good, provided that the truncation radius and the damping parameter are carefully chosen. © 2001 American Institute of Physics. [DOI: 10.1063/1.1364638]

## I. INTRODUCTION

In condensed matter calculations and simulations, one of the most frequently occurring problems is the evaluation of the Coulomb potential, involving the slowly convergent  $r^{-1}$  summation. This problem has received considerable attention throughout the last century, starting from the proposal of the Ewald method,<sup>1</sup> which made the calculation feasible for any periodic system and has long been the most used for evaluating energies, forces, and stresses in the simulation of liquids and solids. The Ewald method assumes that the considered system is periodic, and its application to liquids or in general to disordered systems has long been criticized,<sup>2</sup> as it would create unphysical correlations, but even its application to crystals could be questionable. Indeed, although in principle fully converged Ewald sums yield the correct limiting value of the Coulombic energy, in practice the direct space sums are usually evaluated by including all the charges of a suitable number of replicas of the simulated system. In most cases the system is contained in a parallelepiped, or in a space-filling three-dimensional cell (never possessing spherical symmetry), and the reciprocal space sums run over a more or less large number of reciprocal cells which in the whole are not spherically symmetrical [see Eq. (6) below]. On the other hand, Coulomb potential does show spherical symmetry, as interactions between charges are central forces. Recently, a long article was published by Wolf *et al.*<sup>2</sup> where a comprehensive and deep analysis of the problem is reported, and a new method using just a spherically truncated, pairwise  $r^{-1}$  summation is proposed and verified for a few classical ionic systems, namely NaCl and MgO in crystalline and liquid phase. In the present paper the application of this method to the simulation of complex systems containing charged particles, in particular anhydrous and hydrated microporous aluminosilicates (namely zeolites) and liquid water, which are currently studied by our research group,<sup>3,4</sup> is considered. The chemical composition of zeolites<sup>5,6</sup> usually

consists of silicon, aluminum, oxygen, and exchangeable cations. The crystalline framework is built up by corner sharing  $\text{TO}_4$  tetrahedra (in which the  $T$  sites are occupied by either silicon or aluminum) giving rise to a rather complex but precisely repetitive atomic network with regular cavities joined by channels in which guest molecules of appropriate size can be accommodated. These void interior spaces can admit water, many gases, larger molecules, and cations (usually metallic) which compensate for the charge deficit due to the aluminum/silicon substitution. Although the method proposed in Ref. 2 is simple to implement in energy minimization or molecular dynamics (MD)<sup>7</sup> computer codes, the criteria for the choice of the involved parameters had to be refined for systems with special features like, for instance, noncubic unit cells. It will be shown that not only is it possible to find out general empirical criteria for the estimation of the best parameter values, but also the new method improves the efficiency of the computations without requiring, for the considered systems, any substantial change in their size. Before describing particular applications the main features of the new method will be briefly recalled.

## II. THEORY AND MODEL

### A. The pairwise, spherically truncated $r^{-1}$ sum

After Wolf *et al.*,<sup>2</sup> “the key observation is that the problems encountered in determining the Coulomb energy by pair wise, spherically truncated  $r^{-1}$  summation are a direct consequence of the fact that the system summed over is practically never neutral.” Then the authors proceed to develop the new method by the following steps.

(i) Neutralization of the net charge of the system contained in a sphere with radius  $R_c$ .

It is shown that the total Coulombic energy might be more convergent to the Madelung energy (its limit value) if only a charge-neutralizing potential associated with the net system charge is subtracted from the total energy. This charge-neutralizing potential is evaluated by considering that the charges necessary to neutralize the actual net charge con-

<sup>a)</sup>Electronic mail: pino@uniss.it

tained in a sphere with radius  $R_c$  are always located within the surface shell of thickness  $|\mathbf{b}|$  around  $R_c$ , given that  $|\mathbf{b}|$  represents the nearest-neighbor distance between ions of opposite charge. Therefore, by supposing that  $|\mathbf{b}| \ll R_c$  it is assumed that the entire neutralizing charge is localized *exactly* at the system surface at  $R_c$ .

The charge-neutralization term can be written as follows:

$$E_{\text{tot}}^{\text{neutr}}(R_c) \approx \frac{1}{2} \sum_{i=1}^N \frac{q_i \Delta q_i(R_c)}{R_c} = \frac{1}{2} \sum_{i=1}^N \sum_{\substack{j=1 \\ (r_{ij} < R_c)}}^N \frac{q_i q_j}{R_c} \quad (1)$$

because the net charge within the spherical truncation shell is given by

$$\Delta q_i(R_c) = \sum_{\substack{j=1 \\ (r_{ij} < R_c)}}^N q_j. \quad (2)$$

Like in Ref. 2 it is important to note that the term  $j=i$  needs to be included so that the true total charge in the spherically truncated volume is obtained.

(ii) The ‘‘shifted Coulomb pair potential.’’ After some algebra, it is shown that the direct sum truncated at  $R_c$  minus the neutralizing potential is equivalent to the pairwise sum of ‘‘shifted’’ Coulomb pair potentials  $V_{\text{sh}}^C(r_{ij})$ :

$$V_{\text{sh}}^C(r_{ij}) = q_i q_j \left( \frac{1}{r_{ij}} - \frac{1}{R_c} \right) = \frac{q_i q_j}{r_{ij}} - \lim_{r_{ij} \rightarrow R_c} \left\{ \frac{q_i q_j}{r_{ij}} \right\} \quad (3)$$

from which a sort of ‘‘self term’’ is subtracted. In Eq. (3),  $r_{ij}$  is the distance between the ions  $i$  and  $j$  bearing the charges  $q_i$  and  $q_j$ , respectively. The second form of  $V_{\text{sh}}^C(r_{ij})$  is convenient in order to evaluate the appropriate derivatives when computing the forces, the stresses, etc. Indeed (see Ref. 2 for more details), in order to obtain correct results, derivatives must be evaluated prior to taking the limit. The resulting expression for the total Coulomb energy is

$$E_{\text{tot}}^{\text{Mad}}(R_c) \approx \frac{1}{2} \sum_{i=1}^N \sum_{j \neq i (r_{ij} < R_c)} V_{\text{sh}}^C(r_{ij}) - \frac{1}{2R_c} \sum_{i=1}^N q_i^2, \quad (4)$$

where  $N$  is the total number of ions of the system. Using this approximation of the Madelung energy, for sufficiently large  $R_c$  a convergence toward the limiting value is achieved, which is reasonable but not yet satisfactory.

(iii) The ‘‘damped, charge-neutralized Coulomb pair potential.’’ In order to improve the convergence and make it close to that of the Ewald sum, a damping is applied to the charge-neutralized Coulomb potential, ‘‘in analogy to the trick applied [...] to derive the Ewald sum’’ as it is written in Ref. 2. The final formula is given by

$$E_{\text{tot}}^{\text{Mad}}(R_c) \approx \frac{1}{2} \sum_{i=1}^N \sum_{j \neq i (r_{ij} < R_c)} \left( \frac{q_i q_j \text{erfc}(\alpha r_{ij})}{r_{ij}} - \lim_{r_{ij} \rightarrow R_c} \left\{ \frac{q_i q_j \text{erfc}(\alpha r_{ij})}{r_{ij}} \right\} \right) - \left( \frac{\text{erfc}(\alpha R_c)}{2R_c} + \frac{\alpha}{\pi^{1/2}} \right) \sum_{i=1}^N q_i^2 \quad (5)$$

where  $\text{erfc}$  is the complementary error function,  $\alpha$  is a parameter to be optimized, and the other quantities are defined above. This expression is surprisingly simple and involves only a direct pair summation over the distances with cutoff radius  $R_c$  and constant terms. For comparison, we recall the Ewald summations which, using the same symbols as in Eq. (5), read

$$E_{\text{tot}}^{\text{Mad}} \approx \frac{1}{2} \sum_{i=1}^N \sum_{j=1}^N \sum_{\mathbf{n}=\mathbf{0}}^{\infty} \left( \frac{q_i q_j \text{erfc}(\alpha |\mathbf{r}_{ij} + \mathbf{n} \cdot \mathbf{L}|)}{|\mathbf{r}_{ij} + \mathbf{n} \cdot \mathbf{L}|} \right) - \frac{\alpha}{\pi^{1/2}} \sum_{i=1}^N q_i^2 + \frac{2\pi}{3V} \left( \sum_{i=1}^N q_i \mathbf{r}_i \right)^2 + \frac{2\pi}{V} \sum_{\mathbf{k} \neq \mathbf{0}} \frac{\exp(-k^2/4\alpha^2)}{k^2} Q(\mathbf{k}). \quad (6)$$

In Eq. (6), neglecting the symbols defined previously, the vector  $\mathbf{n}=(n_x, n_y, n_z)$  denotes the three-dimensionally periodic images of the simulation box of sides  $\mathbf{L}=(L_x, L_y, L_z)$  and  $\mathbf{k}$  is a reciprocal space vector. If the cell does not have orthogonal sides the dot product  $\mathbf{n} \cdot \mathbf{L}$  is to be intended as a generalized one giving the correct cell translations in Cartesian coordinates. In the first term, for  $\mathbf{n}=\mathbf{0}$  must be  $j \neq i$ . The function  $Q(\mathbf{k})$  is the so-called charge structure factor, given by

$$Q(\mathbf{k}) = \left( \sum_{j=1}^N q_j \exp[i(\mathbf{k} \cdot \mathbf{r}_j)] \right) \left( \sum_{j=1}^N q_j \exp[-i(\mathbf{k} \cdot \mathbf{r}_j)] \right). \quad (7)$$

The third term in Eq. (6), resulting from the reciprocal space part of the Ewald sums for  $\mathbf{k}=\mathbf{0}$ , is denoted as a ‘‘dipolar term’’ and in most cases (and also in this work) is neglected, because it is zero by symmetry or very small. Usually, the simulation box dimensions and the value of  $\alpha$  are assumed as large so as to ensure that the first term of the Ewald summations converges even for  $\mathbf{n}=\mathbf{0}$ , so that the sums run over all the ions of the simulation box alone. In this case, the terms not containing  $R_c$  in Eq. (5) are of the same analytical form as the first two terms in Eq. (6), but in Eq. (5) only the interionic distances  $r_{ij} < R_c$  are considered. As shown in Sec. V of Ref. 2, *the first double summation in Eq. (5) is numerically very close to the first real-space term of the Ewald sum for the same system and the same damping parameter  $\alpha$ , but including all the ions of the simulation box* (see also Table II). The evaluation of the forces and other quantities related to the derivatives of the potential, which are required for energy minimization or molecular dynamics simulations, is performed starting from Eq. (5) with the above recalled prescription of taking the limit for  $r_{ij} \rightarrow R_c$  after computing the derivatives (see Ref. 2 for details).

## B. Derivation when the spherical truncation volume exceeds the simulation box

One of the most interesting features of the new method is the possibility of using values of  $R_c$  larger than one half of the minimum cell side. In Ref. 2 this statement is implicit but, as it might appear paradoxical, it deserves treatment in detail, also because it allows, in practice, one to achieve remarkable computer efficiency improvements. Obviously,

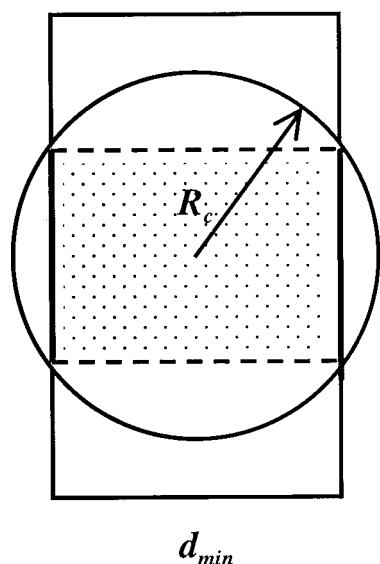


FIG. 1. Two-dimensional representation of the situation when the spherical truncation volume exceeds the simulation box. The system is all contained in the rectangle, and the charges to be included in the evaluation of the Madelung energy are those at a distance less than  $R_c$  from the center of the rectangle. The subsystem contained between the broken lines (in the shaded region) must be neutral. If it is not so, the broken lines are supposed to be slightly deformed (letting their ends unchanged) in order to make the subsystem neutral in any case.

for crystals and liquids, when assuming  $R_c > d_{\min}/2$ , where  $d_{\min}$  is the smallest simulation box side, the minimum image convention and the periodic boundary conditions are retained. Let  $i$  be an ion which, following the minimum image convention, is at the center of the simulation box. Referring to Fig. 1, where a schematic two-dimensional representation of a rectangular simulation box is reported, the choice of  $R_c > d_{\min}/2$  corresponds to include in the evaluation of the Coulombic energy all the point charges contained both in the rectangle and in the circle, by excluding those not contained in the rectangle. If the total net charge is not zero, one can evaluate the charge neutralization energy as follows. First, one can select  $M$  point charges contained between the broken lines in Fig. 1, or, in general, between arbitrary lines connecting the intersections between the rectangle and the circle, so that this subsystem is neutral. In three dimensions, these lines become surfaces with the same properties; the rectangle and the circle become a parallelepiped and a sphere, respectively. Then, if it is assumed, as was previously the case, that the entire neutralizing charge is localized *exactly* at the system surface at  $R_c$ , or better at that portion of the surface which is included in the simulation box, the neutralization energy can be evaluated by again using Eq. (1), but in this case the net charge  $\Delta q_i(R_c)$  is given by

$$\Delta q_i(R_c) = \sum_{j=1}^{N-M} q_j \quad (8)$$

$(r_{ij} < R_c)$

because only the  $N-M$  charges exceeding the above-defined neutral subsystem are to be considered. In order to recover the exact form of Eq. (1), which is necessary to derive the

other formulas of the Wolf method [Eqs. (3)–(5)], a simple trick can be applied. Since the subsystem containing the  $M$  charges is neutral and it is completely included in the truncation sphere, Eq. (8) can be rewritten in the following form:

$$\Delta q_i(R_c) = \sum_{j=1}^M q_j + \sum_{j=1}^{N-M} q_j = \sum_{j=1}^N q_j, \quad (9)$$

$(r_{ij} < R_c)$        $(r_{ij} < R_c)$

which is identical to Eq. (2). Obviously, this derivation holds for any shape of the simulation box. Therefore, the Wolf method can be applied even if  $R_c > d_{\min}/2$ . Indeed, we verified numerically that the Coulombic energy is practically the same (within very small error bounds due to the different number of neutralizing charges that are shifted to the spherical truncation surface) in the whole interval if  $d_{\min}/2 < R_c < R_{\max}$ , where  $R_{\max}$  is one half of the largest diagonal of the simulation box, whatever its shape may be (see also Table II). In the case  $R_c = R_{\max}$ , when  $R_c$  becomes the radius of the sphere circumscribing the simulation box, all the ions of the system are included, so that the system is neutral, and the computed Coulomb energy is exactly the same as the direct part of the Ewald sums (it is easily shown that in this case the neutralizing potential is zero). However, *forces* and *stresses* are not the same, because the direct part of the Ewald sums shows a discontinuity at  $r_{ij} = R_c$ , while the new shifted potential does not (see Sec. VB of Ref. 2). Using forces and stresses as derived by the Wolf method ensures that corrected results are obtained. Moreover, it should be remarked that in this case the symmetry of the system is no more spherical, so that the *forces* and *stresses* derived by the Wolf method should be influenced by the shape of the simulation box, by assuming its translational symmetry. However, this result, at least for *crystals*, turns into an *advantage*, especially if the unit cells are large. Indeed, a spherical truncation which does not include at least one full crystallographic cell cannot account for the translational symmetry of the crystal itself, so that a simulation box made of adjacent unit cells should include at least eight cells to adopt a truncation sphere embedding at least one full unit cell without reaching the simulation cell boundaries. On the other hand, if the unit cell is as large as the ones of some systems considered in this paper (sides of about 2 nm), using  $R_c = R_{\max}$  would allow one to take into account the translational symmetry of a crystal by adopting a relatively small simulation box, resulting in a large reduction of CPU time and storage requirements. As reported in the following, these findings were carefully and successfully verified. A similar approach can be followed to derive another more extensive and interesting property of the Wolf method, which is reported in Sec. VIII of Ref. 2: “Our method is particularly powerful for the simulation of interfacial systems, such as bicrystals, free surfaces, and liquid-vapor interfaces.” Indeed, the treatment is the same except for avoiding the minimum image convention across the interfaces. In conclusion, *the Wolf method allows turning the long-ranged Coulomb interactions into spherically symmetric, relatively short-ranged effective potential functions, like, for instance, the Lennard-Jones ones.*

### C. Evaluation and optimization of the parameters

The parameters required for applying the Wolf method [see Eq. (2)] are the cutoff radius  $R_c$  and the damping parameter  $\alpha$ . The cutoff radius depends in turn on the interionic distance  $|\mathbf{b}|$ , since it must obey the condition  $R_c \gg |\mathbf{b}|$ . Therefore the most general criteria to choose the appropriate values of these parameters should be found. In Ref. 2, the new method was tested for NaCl and MgO in different states (crystal, disordered solid, and liquid) and at different temperatures, and, overall, satisfactory results were achieved for  $1.5a \leq R_c \leq 2.5a$ , where  $a$  is the (cubic) crystallographic cell side, and for  $1.5/a \geq \alpha \geq 0.8/a$ , provided that  $\alpha R_c \approx 2.3$ . By considering the actual interionic distance  $|\mathbf{b}|$  in the two systems, it appears that  $R_c \gg |\mathbf{b}|$  is in practice satisfied for  $R_c \geq 5|\mathbf{b}|$ . Therefore, for systems with  $|\mathbf{b}|$  shorter than in NaCl and in MgO,  $R_c$  could be smaller. This happens for instance for water ( $|\mathbf{b}| \approx 0.1$  nm) and for SiO<sub>2</sub> polymorphs, including zeolites ( $|\mathbf{b}| \approx 0.16$  nm), entailing  $R_c \approx 0.5$  nm and  $R_c \approx 0.8$  nm, respectively. These values are smaller than one half of the usual simulation box dimensions adopted for MD simulations for both kinds of systems, so that they could remain unchanged if the new method is used. However, while for liquid water a cubic simulation box is almost the rule, often unit cells of zeolites are not cubic and have different cell sides, so that there is no “natural” value for  $R_c$  and its right value, as small as possible to limit computational effort, but sufficiently large to ensure convergence, must be found. As a first test, we tried to apply the new method to silicalite<sup>8</sup> which at room temperature shows a monoclinic (but with  $\beta = 90.67^\circ$ ) relatively flat cell so that the simulation box is usually made of two crystallographic cells superimposed along  $c$  with dimensions  $2.0076 \times 1.9926 \times 2.6802$  nm, including 576 atoms. Its framework structure comprises two different channel systems, each defined by ten-membered rings of SiO<sub>4</sub> tetrahedra. Straight channels with an elliptical cross section of approximately 0.57–0.52 nm are parallel to the crystallographic axis  $b$  and sinusoidal channels with nearly circular cross section of 0.54 nm run along the crystallographic axis  $a$ . The resulting intersections are elongated cavities up to 0.9 nm in diameter. For  $R_c = 0.9963$  nm (one half of the *shortest* side, a value which should be sufficiently large according to the above-mentioned arguments), the comparison of the new method results with those of Ewald seemed to be satisfactory. However, the optimum value of  $\alpha$  had to be found. In other cases the meaning of the minimum interionic distance  $|\mathbf{b}|$  becomes unclear. An example is anhydrous zeolite Ca A.<sup>9</sup> The pore system of A-type zeolites could be schematically represented by a cubic array of nearly spherical cavities ( $\alpha$  cages) interconnected through eight-membered oxygen rings (windows) with free aperture about 0.43 nm when not blocked by a cation. The diameter of the  $\alpha$  cages is about 1.12 nm, and in Ca A zeolite the Ca<sup>2+</sup> cations are located near their surface. The Ca<sup>2+</sup> cations neutralize an electron excess arising from the presence of Al atoms instead of Si in TO<sub>4</sub> tetrahedra but spread among several Al, Si, and O atoms of the framework which are not chemically bound to the cations (their distance from the cation is in the range 0.23–0.31 nm), so that a definite value of  $|\mathbf{b}|$  is lacking, and the validity of the new

method in such cases had to be checked. Therefore, we undertake an extended investigation for different systems and different simulation boxes in order to find the correct value of  $|\mathbf{b}|$ , which entails an estimate of the cutoff radius. Among zeolites, we considered silicalite, an all-silica zeolite showing a noncubic unit cell (see the previous text), anhydrous zeolite Ca A,<sup>9</sup> whose unit cell is cubic but with a not well-defined value of  $|\mathbf{b}|$ , and scolecite,<sup>10</sup> which not only contains Ca<sup>2+</sup> cations in a noncubic cell, but also water molecules. Scolecite is a natural fibrous zeolite, which has channels running along the  $c$  direction formed by eight-membered rings of (Si, Al)O<sub>4</sub> tetrahedra. The unit cell is monoclinic, with  $a = 0.65222$  nm,  $b = 1.89678$  nm,  $c = 0.98398$  nm, and  $\beta = 109.97^\circ$ , containing 60 framework atoms (40 O, 12 Si, and 8 Al) and 4 charge compensating Ca<sup>+</sup> ions occupying crystallographically ordered sites in the channels. Three molecules of water for each cation (or 12 molecules per unit cell) are present in the channels in ordered positions and are linked to the cations by electrostatic forces and to the framework by hydrogen bonds, so that diffusion is hindered at room temperature. Finally, liquid water was simulated by using a model recently developed by our research group<sup>4</sup> including the electric field gradient at the position of each oxygen atom, which requires considerable computer resources. The characteristics of the simulated systems and of the simulations are collected in Table I. In particular, in order to check the dependence of the results on  $R_c$  and on the dimensions of the system and to find the optimum value of  $\alpha$ , for silicalite and zeolite Ca A the simulations were performed both for the usual MD boxes (with sides of approximately 2–2.5 nm) and for larger boxes (with sides of about 4–5 nm). Most of the interaction potentials developed in our laboratory for zeolites and water (always assuming that all the particles bear electric charges) are reported or referenced in Ref. 4; the only not yet published parameters are those of the Ca<sup>2+</sup>–water potential functions, which are of the form

$$V_{\text{CaO, H}}(r) = \frac{1}{4\pi\epsilon_0} \frac{q_{\text{Ca}}q_{\text{O, H}}}{r} + A_{\text{CaO, H}} \exp(-b_{\text{CaO, H}}r) + \frac{C_{\text{CaO, H}}}{r^2}, \quad (10)$$

where  $q_{\text{Ca}}$  is the nominal charge of Ca<sup>2+</sup> ( $2e$ ),  $q_{\text{O}} = -0.65966e$ , and  $q_{\text{H}} = 0.32983e$ . The values of the parameters are:  $A_{\text{CaO}} = 2.598 \times 10^5$  kJ mol<sup>-1</sup>;  $A_{\text{CaH}} = 1.2026 \times 10^5$  kJ mol<sup>-1</sup>;  $b_{\text{CaO}} = 0.351$  nm<sup>-1</sup>;  $b_{\text{CaH}} = 0.679$  nm<sup>-1</sup>;  $C_{\text{CaO}} = 15.91$  kJ mol<sup>-1</sup> nm<sup>-2</sup>;  $C_{\text{CaH}} = 8.16$  kJ mol<sup>-1</sup> nm<sup>-2</sup>. The general behavior of the Coulombic energy obtained by the Wolf method using Eq. (5) may be investigated by evaluating the derivative of the Madelung energy with respect to  $\alpha$ :

$$\frac{\partial E_{\text{tot}}^{\text{Mad}}}{\partial \alpha} = \frac{1}{\pi^{1/2}} \left( \sum_{i=1}^N \sum_{j(r_{ij} < R_c)} q_i q_j \exp(-\alpha^2 R_c^2) - \sum_{i=1}^N \sum_{j(r_{ij} < R_c)} q_i q_j \exp(-\alpha^2 r_{ij}^2) - \sum_{i=1}^N q_i^2 \right), \quad (11)$$

where we note that the sums over  $j$  now include the value  $i$

TABLE I. Characteristics of the systems considered in this work.

System	Unit cell dimensions (nm and deg)	Simulation box dimensions (nm and deg)	Number of atoms	
Silicalite (monoclinic)	$a=2.0107$	Silicalite (2 cells)	$a=2.0107$	576
	$b=1.9879$ $c=1.3369$ $\beta=90.67$	Silicalite (12 cells)	$b=1.9879$ $c=2.6738$ $\beta=90.67$ $a=4.0152$ $b=3.9852$ $c=4.0203$ $\beta=90.67$	3656
Zeolite Ca A (cubic)	$a=2.4555$	Zeolite Ca A (1 cell)	$a=2.4555$	624
		Zeolite Ca A (8 cells)	$a=4.9110$	4992
Scollecite (monoclinic)	$a=0.652\ 22$	Scollecite (6 cells)	$a=1.956\ 66$	600
	$b=1.896\ 78$ $c=0.983\ 98$ $\beta=109.97$		$b=1.896\ 78$ $c=1.967\ 92$ $\beta=109.97$	
Water	...	$a=2.1752$ (cubic)		1029 (343 molecules)

$=j$ . The first term is identically zero if the system is neutral, and in general it is much smaller than the others; the third term is always negative, so that for large values of  $\alpha$ , when the second term also becomes negligible, the slope of the Madelung energy versus  $\alpha$  is negative. For small values of  $\alpha$  usually (an exception is liquid water, see the following) the first term is negative and the second one is positive, because in ionic materials the particles of opposite charge are closer together than the particle of the same charge. Moreover, the number of nearest neighbors is at least four and for sufficiently small values of  $\alpha$  the Gaussian functions in the first and second terms approach unity. Thus it is likely that their sum is positive and larger than the third term, so that the slope of the Madelung energy is positive. Therefore, it is expected that for a (relatively small) value of  $\alpha$  the Madelung energy shows a maximum. On the other hand, if the direct space Ewald sums in Eq. (6) are limited to the simulation box, that is, the terms with  $\mathbf{n} \neq \mathbf{0}$  are neglected, as usual when the simulation box is sufficiently large, the derivative with respect to  $\alpha$  of the Madelung energy as evaluated using Ewald sums is given by

$$\frac{\partial E_{\text{tot}}^{\text{Mad}}}{\partial \alpha} = \frac{1}{\pi^{1/2}} \left( \sum_{i=1}^N \sum_{j=1}^N q_i q_j \exp(-\alpha^2 r_{ij}^2) - \sum_{i=1}^N q_i^2 \right) + \frac{2\pi}{V} \sum_{\mathbf{k} \neq \mathbf{0}} \frac{\exp(-k^2/4\alpha^2)}{2\alpha^3} Q(\mathbf{k}). \quad (12)$$

The first and second terms in Eq. (12) are similar to the corresponding (second and third, respectively) terms of Eq. (11) and it is easily shown that their behavior too is similar. Therefore, we usually expect that for small values of  $\alpha$ , the contribution of the third term being negligible, the slope of the Madelung energy is positive and decreases until it reaches zero. However, for larger values of  $\alpha$  the third term, representing the contribution of the reciprocal space sums,

grows so that the slope of the Madelung energy maintains the zero value, because this energy becomes constant. In other words, the curve representing the Ewald sums results reaches a plateau and the corresponding Coulomb energy can be assumed as the limiting value of the Madelung energy.

### III. CALCULATIONS, RESULTS, AND DISCUSSION

We evaluated first the Madelung energies for the experimental structures of silicalite ( $1 \times 1 \times 2$  and  $2 \times 2 \times 3$  unit cells), zeolite Ca A ( $1 \times 1 \times 1$  and  $2 \times 2 \times 2$  unit cells), scolecite ( $3 \times 1 \times 2$  unit cells), and water (343 molecules in a cubic box) in order to check the convergence of the values of the energies obtained by Ewald and Wolf methods depending on the values of  $\alpha$  and on  $R_c$ . The cutoff radius  $R_c$  was set equal to one half of the *smallest* and of the *largest* cell sides (when significantly different) for noncubic cells. Moreover, in all cases we also performed a simulation with  $R_c$  equal to the radius of the sphere circumscribing the MD box (see Table I for more details about the considered systems). Figure 2 illustrates an example of the Coulomb energy trend as a function of the damping parameter  $\alpha$ , evaluated from the Ewald method and Wolf method for different values of  $R_c$ . The data refer to zeolite Ca A, the most critical system among those considered in the present study, because of the undefined but possibly large value of  $|\mathbf{b}|$ , which would require a large  $R_c$  for a correct application of the Wolf method. Figure 2(a) shows the results for the smaller simulation box (one crystallographic cell); while in Fig. 2(b) the ones for the larger simulation box (eight crystallographic cells) are reported. It is important to remark that in both cases the trend expected on the basis of the arguments reported in Sec. II C, in particular about Eqs. (11) and (12), is observed. Indeed, for very small values of  $\alpha$  the Coulomb energy resulting from the Ewald sums does not converge to the correct value, but as  $\alpha$  is increased the curve reaches a plateau and the

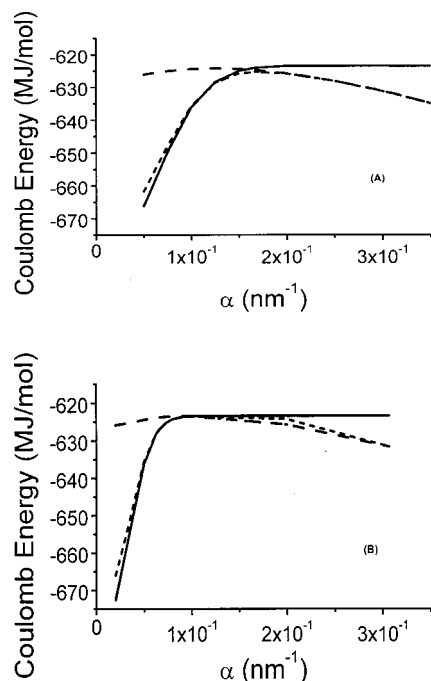


FIG. 2. Total Coulomb energy per crystallographic unit cell for zeolite Ca A (in MJ/mol) as a function of the damping parameter  $\alpha$  (in  $\text{nm}^{-1}$ ) contained in Eq. (5), for different evaluation methods (Ewald: continuous lines; Wolf: broken lines) and for different values of the cutoff radius  $R_c$ . (a) One unit cell; dashed line:  $R_c = d_{\min}/2 = 1.228$  nm; dotted line:  $R_c = (\sqrt{3}/2)d_{\min} = 2.127$  nm. (b) Eight unit cells; dashed line:  $R_c = d_{\min}/2 = 2.455$  nm; dotted line:  $R_c = (\sqrt{3}/2)d_{\min} = 4.254$  nm.

corresponding Coulomb energy can be assumed as the limiting value of the Madelung energy. This trend was observed for all the considered systems, but the value of  $\alpha$  for which the Coulomb energy becomes constant, or the position of the ‘‘knee’’ in the curve, depends on the dimensions of the simulation box. An exception is water, which shows a very small variation of the Coulomb energy obtained by both methods even for very small values of the damping parameter. This effect is caused by the peculiar characteristics of water, which is a structured molecular hydrogen bonded liquid. Indeed, the distribution of the charges surrounding oxygen and hydrogen atoms is different from that of an ionic material or an aluminosilicate, and a detailed inspection of the actual structure of the first neighbors molecular shell is sufficient to ascertain that the derivative of the Madelung energy, given by Eq. (12), is close to zero for any value  $\alpha$ . Before discussing the dependence of the Ewald energy curve on the simulation box dimensions, the results of the Wolf method will be illustrated. Referring again to Fig. 2, for  $R_c = d/2$  ( $d$  is the cubic cell side) and for small values of  $\alpha$  the Coulomb energies are closer to the limiting value than the ones derived from the Ewald sums. They increase slightly for increasing  $\alpha$ , reaching a maximum approximately in correspondence with the knee of the Ewald sums curve. For higher values of  $\alpha$  the Coulomb energies yielded by the Wolf method decrease monotonically diverging from the limiting value of the Ewald sums, as expected on the basis of the discussion of the behavior of Eq. (11). For the smaller simulation box this effect is greater than for the larger simulation box. However, for a given system, the decrease of the Coulomb energies for

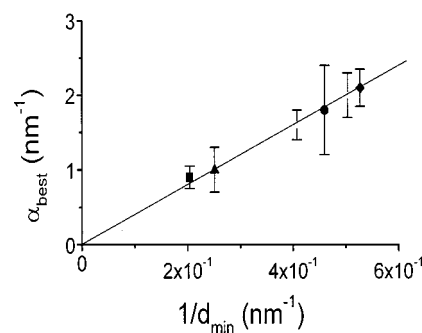


FIG. 3. Minimum value of the damping parameter  $\alpha$  (in  $\text{nm}^{-1}$ ) ensuring the correct convergence of the Coulomb energy both for Ewald sums and the Wolf method for the systems considered in this work as a function of  $1/d_{\min}$  (in  $\text{nm}^{-1}$ ), where  $d_{\min}$  is the smallest simulation box side. Black square: zeolite Ca A (8 cells); black triangle: silicalite (12 cells); gray square: zeolite Ca A (1 cell); gray triangle: silicalite (1 cell); circle: water; diamond: scolecite.

increasing  $\alpha$  yielded by the Wolf method is practically independent of  $R_c$ . This trend is to be expected because, following the arguments of Sec. II C, Eq. (11), the limit value of the derivative of the Madelung energy for large  $\alpha$  is independent of  $R_c$ . We stress that the above-described behavior is shown by all the considered systems, so that a general rule may be guessed: *there is always an optimum value of  $\alpha$ ,  $\alpha_{\text{best}}$ , for which not only the results of the two methods are close together but also both of them yield the correct Coulomb energy value (which can be evaluated by the full converged Ewald sum for large  $\alpha$ ), provided that  $R_c$  is sufficiently large, in order to satisfy the condition  $R_c \gg |\mathbf{b}|$ .* Because  $\alpha$  must be as small as possible,  $\alpha_{\text{best}}$  should correspond to the knee in the Ewald results curve. It remained to find another rule relating  $\alpha_{\text{best}}$  to some characteristic of the system, in order to avoid the evaluation of Coulomb energy versus  $\alpha$  curves in each case. By comparing the results reported in Figs. 2(a) and 2(b), and the corresponding trends for the smaller and larger simulation boxes of silicalite (not shown), it appeared that  $\alpha_{\text{best}}$  decreased by increasing the dimensions of the simulation boxes *independently of  $R_c$* . Therefore, we attempted to plot the values of  $\alpha_{\text{best}}$  against the inverse of some measure of the simulation box dimensions. It was found that the best results were obtained by considering *the smallest side of the simulation box*. The results are shown in Fig. 3, where it appears that for all the considered systems the dependence of  $\alpha_{\text{best}}$  on  $1/d_{\min}$ , where  $d_{\min}$  is the smallest simulation box side, was represented very well by a straight line. The best reproduction of the Ewald results was obtained for  $\alpha_{\text{best}} = 4/d_{\min}$ , within an error of a few percent. We did not succeed in showing that this result can be derived analytically from Eq. (11). However, it is easy, though a bit tedious, to verify that for a perfect rock salt structure crystal, assuming a cubic box of side  $d = d_{\min} = 10|\mathbf{b}|$ ,  $\alpha = 4/d_{\min} = 2/(5|\mathbf{b}|)$ , and  $R_c \geq 5|\mathbf{b}|$ , Eq. (11) yields a value very close to zero as a result of the sum of relatively large mutually canceling terms. On the basis of these findings, we performed a series of test MD simulations in the *NVE* ensemble of the considered systems (see Table I). The systems were all equilibrated at a nominal temperature of 300 K and the pro-

TABLE II. Results of MD simulations for the systems considered in this work. By “direct Coulomb energy” we mean for the Ewald method the real space sums; for the Wolf method the first double sums in Eq. (5). Direct and total Coulomb energies are per crystallographic unit cells (for water per simulation box). The CPU time includes the contribution of short-range interactions, and its value is relative to the one necessary for the simulations with the Ewald method. For the larger systems the CPU time relative to the corresponding smaller systems is also reported (in parentheses).

System	Number of simulation	Method (E=Ewald) (W=Wolf)	Damping parameter $\alpha$ (nm <sup>-1</sup> )	Cutoff radius $R_c$ (nm)	Direct Coulomb energy (MJ/mol)	Total Coulomb energy (MJ/mol)	Pressure (MPa)	Percent rms total energy	Relative CPU time
Silicalite (2 cells)	1	E	2.0	...	-273.452	-363.634	30	$0.40 \times 10^{-4}$	1.00
	2	W	2.0	0.994	-273.267	-363.765	162	$0.16 \times 10^{-3}$	0.73
	3	W	2.0	1.340	-273.399	-363.705	38	$0.35 \times 10^{-4}$	0.75
	4	W	2.0	1.948	-273.412	-363.713	51	$0.42 \times 10^{-4}$	0.96
Silicalite (12 cells)	5	E	1.006	...	-318.387	-363.809	122	$0.15 \times 10^{-4}$	1.00(20.8)
	6	W	1.006	1.988	-318.189	-363.705	4	$0.12 \times 10^{-4}$	0.69(14.5)
	7	W	1.006	3.483	-318.357	-363.778	24	$0.16 \times 10^{-4}$	0.85(17.9)
	8	W	2.0	1.948	-273.334	-363.447	52	$0.63 \times 10^{-5}$	0.68(14.1)
	9	W	1.006	0.994	-313.929	-365.685	100	$0.28 \times 10^{-2}$	0.54(11.2)
	10	W	2.012	0.994	-272.766	-363.746	3	$0.98 \times 10^{-4}$	0.54(11.2)
	11	W	1.006	1.340	-317.651	-364.761	-1468	$0.38 \times 10^{-3}$	0.57(11.9)
	12	W	1.492	1.340	-296.242	-363.746	0	$0.31 \times 10^{-2}$	0.57(11.9)
Zeolite Ca A (1 cell)	13	E	1.629	...	-483.729	-621.864	-1397	$0.13 \times 10^{-1}$	1.00
	14	W	1.629	1.228	-483.173	-621.613	-1138	$0.34 \times 10^{-3}$	0.53
	15	W	1.629	2.127	-483.829	-622.094	-1264	$0.33 \times 10^{-3}$	0.91
Zeolite Ca A (8 cells)	16	E	0.814	...	-552.753	-621.721	-1455	$0.47 \times 10^{-2}$	1.00(71.4)
	17	W	0.814	2.455	-552.131	-621.366	-1492	$0.13 \times 10^{-1}$	0.69(50.0)
	18	W	0.814	4.254	-552.633	-621.721	-1439	$0.32 \times 10^{-2}$	0.85(62.5)
	19	W	1.629	2.127	-482.943	-621.204	-1291	$0.45 \times 10^{-1}$	0.63(45.0)
	20	W	0.814	1.228	-544.586	-623.562	-4905	$0.39 \times 10^{-2}$	0.54(38.5)
	21	W	1.629	1.228	-483.019	-621.565	-1477	$0.24 \times 10^{-3}$	0.54(38.5)
Scolecite (6 cells)	22	E	2.1	...	-51.8204	-70.947	-699	0.21	1.00
	23	W	2.1	0.984	-51.7279	-70.889	-940	0.23	0.26
	24	W	2.1	1.866	-51.7765	-70.909	-829	0.12	0.32
Water (liquid)	25	E	1.839	...	-155.141	-187.302	648	$0.65 \times 10^{-3}$	1.00
	26	W	1.839	1.088	-154.962	-187.401	872	$0.28 \times 10^{-2}$	0.37
	27	W	1.839	1.884	-155.145	-187.418	677	$0.83 \times 10^{-3}$	0.39

duction trajectory was  $10^4$  steps long, corresponding to 10 ps for the anhydrous zeolites and to 5 ps for scolecite and water. This time proved to be sufficient for the estimation of the quantities we were interested in: average Madelung energy and contribution of the “direct sum” for both Ewald and Wolf methods, the total energy conservation, expressed as rms percent variation, and, finally, the ratio of the CPU time required for the calculation using the two methods. Moreover, the average structures and the vibrational spectra were evaluated following standard procedures (see Ref. 3, and references therein). The most relevant results are collected in Table II, where the simulations are numbered in order to make the discussion easier. First, it was assumed  $\alpha = 4/d_{\min}$  and, in order to check the dependence of the results on  $R_c$ , the simulations were repeated by increasing the value of  $R_c$  from  $d_{\min}/2$  to the radius of the sphere circumscribing the simulation box (simulations 2, 4, 6, 7, 14, 15, 17, 18, 23, 24, 26, and 27). As evidenced in Sec. II B, when assuming  $R_c > d_{\min}/2$ , the minimum image convention and the periodic boundary conditions were retained. For the smaller simulation box of silicalite, the simulation was performed also by assuming  $R_c$  equal to the *largest* cell side (simulation 3). Moreover, for silicalite and zeolite Ca A, simulations of the

*larger* systems were carried out for  $R_c$  equal to the radius of the sphere circumscribing the *smaller* simulation box and for the value of  $\alpha$  corresponding to the smaller simulation box, in order to compare the results of systems with the truncation sphere completely embedded in the simulation box with those of corresponding neutral simulation boxes completely contained in the truncation sphere with the same  $R_c$  (simulations 8 and 19 to be compared with simulations 4 and 15, respectively). The Ewald method should yield the same results for the same systems with different simulation boxes. Therefore, their actual differences can be considered as an intrinsic numerical error, *which in the following discussion is assumed as a measure of the goodness of the results*. For instance, the relative difference between the total Coulomb energy for the smaller and larger simulation boxes of silicalite (simulations 1 and 5, respectively) and of zeolite Ca A (simulations 13 and 16, respectively) is about  $10^{-2}\%$ . Therefore we consider “satisfactory” all the total Coulomb energies obtained by simulations performed using the Wolf method yielding differences within  $10^{-2}\%$  from the ones evaluated by the Ewald method for the same system, and “not quite satisfactory” (although possibly acceptable) the others. It is clearly shown that for the above-considered

simulations, to be compared with simulations 1, 5, 13, 16, 22 and 25, which were performed using the Ewald summations, the two methods yield practically the same values of the Coulomb energy (within about  $10^{-2}\%$ ), both for the total one and the “direct” contribution, which for the Wolf method is to be intended as the first double sum in Eq. (5), as remarked previously. This is true also for the smaller simulation box of zeolite Ca A with  $R_c = d_{\min}/2$ . The general trend of the structural results, which for crystals include the distribution of the atomic coordinates (taking into account the symmetry of the system)<sup>3</sup> and the corresponding averages, while for water consist of radial distribution functions and average molecular dimensions, is similar for the two methods. For water the results are practically indistinguishable whereas for crystals, in spite of the built-in translational symmetry of the Ewald sums, the Wolf method yields more symmetric and ordered structures in all the considered cases (except for the smaller simulation box of silicalite with  $R_c = d_{\min}/2$ ). This is not surprising, because, as remarked in Sec. I, the Wolf method retains the spherical symmetry of the Coulomb potential, while Ewald sums do not. Therefore, the Wolf method should be more suitable, not only for liquids and disordered systems, but, almost paradoxically, also for crystals. The simulation runs were too short for a reliable evaluation of the pressure, which is the most critical quantity for the Wolf method. This problem was evidenced in the original paper<sup>2</sup> where a corrective term was also derived for liquids. However, its value for water ( $-5.3$  MPa), is not sufficient to completely reduce the gap between the values obtained by the two methods, although for the larger value of  $R_c$  the difference is less than 5%, an encouraging result. A more irregular trend is observed for crystals, where differences of the order of 100 MPa among the computed pressures of each system are found. We note in passing that the large negative values for zeolite Ca A is to be expected, as this structure in its equilibrium state is hydrated, while for scolecite it is caused probably by a water–zeolite potential which is too deep and, indeed, is under revision. The vibrational spectra evaluated using the two methods are very similar; in particular, the ones obtained with the Wolf method for the smaller systems are practically the same as the corresponding spectra resulting from the Ewald method for the larger systems, when available. In summary, it appears that the Wolf method applied even to the smaller simulation boxes, which correspond to the usually adopted ones for MD calculations, are sufficiently large to yield results reasonably close to the ones obtained by the Ewald method, especially if  $R_c$  corresponds to the radius of the sphere circumscribing the simulation box. In particular, the results for the smaller simulation box of zeolite Ca A show that the condition  $R_c \gg |\mathbf{b}|$  is satisfied even for  $R_c = d_{\min}/2$ . Therefore, it can be assumed that in this case  $|\mathbf{b}|$  is of the order of 0.2 nm, or that it corresponds to the largest of the nearest-neighbor distances (about 0.23 nm) between particles of opposite charge, in spite of the fact that the involved ions (the charge compensating  $\text{Ca}^{2+}$  cations and the oxygen atoms of the framework) do not completely neutralize each other. In some cases, for instance when long-range distribution functions or diffusive properties are to be studied, large simulation boxes must be

used, and a value of  $R_c < d_{\min}/2$  could be sufficient to ensure a correct simulation. A recent example is reported in Ref. 11, where the screening behaviors of molten and gaseous NaCl are studied by assuming  $R_c = a/3$ ,  $a$  being the side of the cubic simulation box. By performing simulations 9 and 11 (for silicalite), and 20 (for zeolite Ca A) we verified that maintaining the value of  $\alpha$  which is the best for the larger simulation boxes leads to results which are not fully satisfactory (in the above-specified meaning). Indeed, in these cases the interactions of each charged particle are cut at  $R_c$ , so that the value of  $\alpha$  cannot be correlated with the dimensions of the simulation box. Instead, it should be related to  $R_c$ , by considering an effective simulation box of side  $d' = 2R_c$  and, therefore,  $\alpha = 2/R_c$ . The results of simulations 10, 12, and 21 show that this choice considerably improves the performances. The computational efficiency of the two methods can be compared by considering the relative CPU time needed for the calculations, besides the consideration of the much simpler form of the algorithm required by the Wolf method. In the Ewald method, the real space summations are performed over all the charged particles of the simulation box, and after the reciprocal space sum is to be added up. Usually, in order to obtain the maximum efficiency, it is suggested to choose a value of  $\alpha$  entailing a roughly equivalent CPU time consumption for each kind of sums; in practice, for the considered systems  $\alpha$  should be of the order of  $0.3 \text{ nm}^{-1}$ , and this value was used in our previous works [Refs. 3 and 4], but no relevant difference in computer time was recorded for smaller values of  $\alpha$ , because the simulation boxes are sufficiently large to allow including a relatively small number of points in the reciprocal space sums even for relatively large values of  $\alpha$ . In the Wolf method, the summations involve the real space only, so that it is expected to be faster. The actual CPU time consumption relative to the Ewald method performances on a HP K-460 computer equipped with four processors are reported in Table II. The Wolf method always appears more efficient, and the computer time is reduced by a factor spanning from about 0.9 (for  $R_c$  corresponding to the radius of the circumscribing sphere in silicalite) to about 0.3 (for scolecite, where the potential model for the included water<sup>4</sup> involves the gradient of the electric field, which requires large computer resources for the evaluation of the reciprocal space part of the Ewald sums.) In Table II, for the larger simulation boxes, the computer time relative to Ewald method calculations of the corresponding smaller simulation boxes is also reported. The  $N^2$  law for computer time (where  $N$  is the number of charged particles) is not exactly obeyed because we report the total CPU time, including the evaluation of short-range forces, input–output operations, and some statistical calculations. For simulations with  $R_c < d_{\min}/2$ , the efficiency could be improved by using neighbor lists.<sup>7</sup> Nevertheless, using the larger simulation boxes, if not necessary, appears to demand too much computer time. The rms deviation of the total energy, which is an index of the accuracy of the calculations, is also reported for each simulation in Table II. It is about of the same order of magnitude for the two methods, without a definite trend, so that the same value of the time step may be used for both methods.



#### IV. CONCLUSIONS

Some conclusions about the simulation of aluminosilicates and water using the Wolf method for the evaluation of Coulombic interactions may be drawn from the present study.

(i) The condition  $R_c \gg |\mathbf{b}|$  (in practice  $R_c \geq 5|\mathbf{b}|$ ) is reasonably satisfied if  $|\mathbf{b}|$  corresponds to the largest of the nearest-neighbor distances between particles of opposite charge. Therefore, simulation boxes with  $d_{\min} = 2R_c \geq 10|\mathbf{b}|$  (where  $d_{\min}$  is the smallest simulation box side) are sufficiently large to obtain results equivalent to those resulting from the Ewald sums by using the Wolf method. In particular, for the systems considered in this work, the usual simulation boxes (with sides of at least about 2 nm) are suitable for both methods.

(ii) In order to ensure a good reproduction of the results obtained by the Ewald method with the Wolf one, if  $R_c \geq d_{\min}/2$  the optimum value of the damping parameter  $\alpha_{\text{best}}$ , within narrow error bounds, is given by  $\alpha_{\text{best}} = 4/d_{\min}$ . If the system is sufficiently large to fit criterion (i) with  $R_c < d_{\min}/2$ , good results are obtained if  $\alpha = 2/R_c$ .

(iii) For a given simulation box and assuming  $\alpha = 4/d_{\min}$ , the best results are obtained with  $R_c$  equal to the radius of the sphere circumscribing the simulation box.

(iv) The computer efficiency is better for the Wolf method. Moreover, as it retains the spherical symmetry of the Coulombic potential, it seems physically more meaningful than the Ewald method not only for liquids and disordered systems, but also for crystals.

In the present paper it is shown that the Wolf method may be used safely for the evaluation of Coulombic interac-

tions in condensed matter simulations not only for purely ionic substances but also for complex systems containing charged particles like anhydrous and hydrated aluminosilicates and liquid water, provided that the involved parameters are chosen following some criteria that we tried to derive. We shall apply this method extensively in the future, and we wish to recommend its use as computationally more efficient and physically more meaningful than the Ewald method.

#### ACKNOWLEDGMENTS

This research is supported by Italian Ministero dell'Università e della Ricerca Scientifica e Tecnologica (MURST), by Università degli studi di Sassari, and by Consiglio Nazionale delle Ricerche.

<sup>1</sup>P. P. Ewald, *Ann. Phys. Z.* **19**, 253 (1921).

<sup>2</sup>D. Wolf, P. Keblinski, S. R. Phillpot, and J. Eggebrecht, *J. Chem. Phys.* **110**, 8254 (1999).

<sup>3</sup>P. Demontis and G. B. Suffritti, *Chem. Rev.* **97**, 2845 (1997).

<sup>4</sup>P. Cicu, P. Demontis, S. Spanu, G. B. Suffritti, and A. Tilocca, *J. Chem. Phys.* **112**, 8267 (2000).

<sup>5</sup>G. Gottardi and E. Galli, *Natural Zeolites* (Springer, Berlin, 1985).

<sup>6</sup>D. W. Breck, *Zeolites Molecular Sieves* (Wiley, New York, 1973).

<sup>7</sup>*Computer Simulations in Chemical Physics*, edited by M. P. Allen and D. J. Tildesley (Kluwer, Dordrecht, 1994).

<sup>8</sup>H. van Koningsveld, J. C. Jansen, and H. van Bekkum, *Zeolites* **10**, 235 (1990), and references therein.

<sup>9</sup>G. Artioli, J. V. Smith, and A. Kvick, *Acta Crystallogr., Sect. C: Cryst. Struct. Commun.* **40**, 1658 (1984).

<sup>10</sup>R. L. Firor and K. Seff, *J. Am. Chem. Soc.* **100**, 91 (1978).

<sup>11</sup>P. Keblinski, J. Eggebrecht, D. Wolf, and S. R. Phillpot, *J. Chem. Phys.* **113**, 282 (2000).